Journal of Polymer Research _####################_
https://doi.org/10.1007/s10965-020-02346-4

ORIGINAL PAPER

# Arapey sweet potato peel waste as renewable source of antioxidant: extraction, nanoencapsulation and nanoadditive potential in films

Beatriz Guerrero-León[1] · Graciela Corbino[3] · Alain Dufresne[5] · María Inés Errea[4] · Norma D'Accorso[1,2] · Nancy L. Garcia[2]

Received: 15 January 2020 / Accepted: 9 November 2020


## Abstract

In this work, the peel of Arapey Sweet Potato (Ipomoea batatas), a vegetable waste, was used as a source of phenolic compounds which are widely recognized as beneficial antioxidants for human health. The extract obtained from Ipomoea batatas exhibited an antioxidant activity significantly higher than many antioxidant agents reported in literature (476.96 mg of TROLOX $mL^{-1}$), as well as good thermal stability. Nanocapsules of the extract coated with low molecular weight polylactic acid were prepared by the emulsification-solvent evaporation method and the nanoparticles obtained were characterized physical; thermal; and morphologically. An analysis of the variables that were investigated to increase the encapsulation efficiency is presented here. Besides, PLA films prepared via the solution-casting method exhibited good compatibility with the nanoparticles loaded with the antioxidant extract, as was evidenced by the uniform and stable dispersion of these particles in the films. Furthermore, an improvement of the mechanical properties of the PLA films due to the presence of the nanoparticles were clearly observed. Results reported here are encourage enough to propose the nanocapsules described in this work as additives or to be used immersed in films for controlled release of antioxidants, putting in value a vegetable waste.

**Keywords** Nanocomposites · Biodegradable · Biopolymers · Antioxidants · Film

## Introduction

Currently, most industries are interested in environmentally friendly, versatile and low-cost raw materials. On the other hand, composite materials are attractive because they combine the properties of different compounds to obtain new materials with improved properties. These materials are particularly interesting when they are obtained from biodegradable polymers and renewable biomass, [1] such as natural antioxidants obtaining from vegetable waste [2–4].Natural antioxidants are primarily phenols synthesized by plants as part of their secondary metabolism [5] and the possibility of obtaining them from plan waste represents an economic advantage. Particularly, we are interested in the peel of Arapey Sweet Potato (*Ipomoea batatas*), a variety widely consumed in Argentina. As a result of the industrialization of this root, tons of peels are generated and discarded annually and, to the author's knowledge, this waste is not currently used. Considering that phenols are very vulnerable to oxidizing environment, they must be encapsulated to improve their storage stability [6].

✉ Norma D'Accorso
norma@qo.fcen.uba.ar

✉ Nancy L. Garcia
nancylis@qo.fcen.uba.ar

[1] Universidad de Buenos Aires, Facultad de Ciencias Exactas y Naturales (FCEyN), Departamento de Química Orgánica, Buenos Aires, Argentina

[2] CONICET- Universidad de Buenos Aires. Centro de Investigaciones en Hidratos de Carbono (CIHIDECAR), Buenos Aires, Argentina

[3] Instituto Nacional de Tecnología Agropecuaria Estación Experimental Agropecuaria San Pedro (INTA), Buenos Aires, Argentina

[4] Instituto Tecnológico de Buenos Aires (ITBA), Buenos Aires, Argentina

[5] Univ. Grenoble Alpes, CNRS, Grenoble INP, LGP2, F-38000 Grenoble, France

Many articles describing encapsulation procedures have been published, in which a wide variety of encapsulation agents are proposed [7–17]. Among them, polylactic acid (PLA) is especially attractive due to its biodegradability and non-toxicity. In addition, due to its interesting physical properties, the use of PLA has become popular and is one of the first options to consider when an environmentally friendly polymer is required for a wide range of applications [13, 18–21].

Considering the above discussion, the aim of this work was to develop and characterize antioxidant-loaded biodegradable PLA films to be used in multiple ways including intelligent packaging, agro-mulching, eco green coatings, among others.

## Materials and methods

### Materials

High molecular weight poly(lactic acid) (PLA) pellets were provided by Shenzhen Bright China Industrial Co., Ltd. (Wuhan, China) (L-LA 90%, 10% D-LA; Mw = 200,000 g $mol^{-1}$; polydispersity index = 1.8) and purified before use by dissolving in dichloromethane and re-precipitating in methanol. Poly (vinyl alcohol) (99 % hydrolyzed, Mw = 89,000 – 98,000 g $mol^{-1}$) was purchased from Sigma-Aldrich (USA). Solvents were reagent grade, and they were dried and distilled before use according to standard procedures. All other reagents were of analytical grade and used without further purification.

### Synthesis of low molecular weight poly (lactic acid) (PLA)

Low molecular weight PLA was synthesized by direct condensation method using a reactor equipped with a vacuum pump and cold traps for removing water using *p*-toluene sulfonic acid as catalyst. The crude product was purified by dissolving in dichloromethane and re- precipitating in methanol[22].

### Molecular weight determinations

PLA molecular weight was determined by Size Exclusion Chromatography (SEC) on a Waters 600 at 31 °C, through a Styragel HR 4 THF- 7.8 x 300 mm - (5K-600K) column and a refractive index detector 2414 at a flow rate of 1 mL $min^{-1}$, using polystyrene standards.

### Preparation of Arapey sweet potato (Ipomoea batatas) peel extract (PExt)

Fresh roots harvested in San Pedro (Buenos Aires) were well cleaned. The peel was carefully removed (50 g) and suspended in methanol (400 mL). The suspension was heated to 80° C for 10 min and then stored under continuous stirring for 24 h at room temperature. After that, the mixture was filtered and the solution containing the antioxidants was evaporated under reduced pressure (extract yield: 4 % of fresh Arapey sweet potato peel). Then, the residue was resuspended in methanol and stored, as a stock solution, at 4°C in a dark flask for further analyses.

### Characterization of the extract

#### Identification and quantification of individual phenolic acids

Analyses were carried out by reversed-phase high performance liquid chromatography (RP-HPLC) using Agilent Series 1200 (Agilent Technologies, USA) system, equipped with an ultraviolet detector. Aliquots of the extract were filtered through a 0.45mm membrane filter. Antioxidant methanolic extract (20 µL) was injected onto a ZORBAX Eclipse XDB-C18.5 µm, 4.6 mm x 250 mm column (Agilent Technology). The gradient elution program was 20% acetonitrile: 80% water (0–10 min), 20–30 % acetonitrile (10–20 min), 30-50 % acetonitrile (20-30 min) at a flow rate of 0.7 mL $min^{-1}$.

The peaks detected were identified and quantified by comparing the retention time and peak area to that of known standards. Quantification was based on absorbance at 320 nm.

#### Determination of antioxidant activity-(DPPH radical inhibition assay)

The antioxidant activity of the extract was estimated according to the procedure described by Brand-Williams et al.[23]

Briefly, a 0.1 mM solution of 2,2-diphenyl-1-picrylhydrazyl (DPPH) in methanol was prepared and 2 mL of this solution was mixed vigorously with different volumes of the methanolic extract PExt (10-50 µL). The samples, by duplicates, were kept at room temperature for 30 min in the dark. Methanol and each sample solution were used as a blank.

Absorbance (A) was measured at 517 nm and the extend of radical scavenging was calculated based on Eq. 1:

$$\%\ \text{Scavenging} = \frac{\text{Ablank} - \text{Asample}}{\text{Ablank}} \times 100 \quad (1)$$





Journal : Large 10965 | Article No : 2346 | Pages : 12 | MS Code : 2346 | Dispatch : 13-11-2020

The IC50 value, defined as the concentration of the sample leading to 50% reduction of the initial DPPH concentration, was obtained from the linear regression of plots of mean percentage of the antioxidant activity against the concentration of the test extracts (μg $mL^{-1}$). Antioxidant capacity of the extract was expressed as: Trolox equivalent antioxidant capacity (TEAC) calculated using Trolox as standard to construct the calibration curve, expressed by TROLOX $mL^{-1}$, [24, 25] where Trolox is the 3, 4-dihydro-6-hydroxy-2, 5, 7, 8-tetramethyl-2H-1-benzopyran-2-carboxylic acid, a widely used antioxidant.

## Preparation of PLA nanoparticles (NP)

PLA nanoparticles were prepared by the emulsification-solvent evaporation method, as previously reported by Rousaki et al. [26]. Briefly, solutions of PLA (Mw=18,000 and 24,500 g $mol^{-1}$) in acetone (10 mg $mL^{-1}$) ( , were added to an aqueous solution of PVA (1 % w $w^{-1}$) and the mixtures were kept at room temperature under magnetic stirring (150 rpm) overnight. After that, low RCF (2683) in a centrifuge (Beckman J2-21M / E, California, USA) at 5°C for 5 min was applied to remove aggregated nanoparticles. The supernatants were separated and further centrifuged at RCF of 10733 at 5 °C for 20 or 40 min. The pellets containing the nanoparticles were washed with Milli-Q water to remove residual solvent and surfactant, re-suspended in 5 mL of water, and stored at 4°C in a dark flask.

## Preparation of antioxidant-loaded PLA nanoparticles ($NP_{PExt}$)

Encapsulation of PExt was carried out following the procedure described above but, in this case, a PExt organic solution was added to an organic solution of PLA and the mixture was added to the aqueous solution of PVA. Different organic solvents were tested.

In order to study the best encapsulation conditions, different experiments were performed modifying the PExt: PLA ratio (0.2:1 or 0.6:1), RCF of 10733 or 18138, centrifugation time (20 or 40 min) and PLA molecular weight ($M_W$ 18,000 or 24,500 g $mol^{-1}$).

### Encapsulation efficiency (EE%)

The amount of PExt entrapped within the nanoparticles was determined indirectly, i.e. by measuring the amount of free PExt in the supernatant recovered after centrifugation, using a UV-Vis spectrometry (Jenway 6705 spectrophotometer). The drug entrapment efficiency (EE %) was expressed as the difference between the amount of PExt in the supernatant relative to the total amount used for the nanoparticle preparation. The supernatant was evaporated at 40°C under reduced pressure and the residue was re-suspended in methanol. After 24 h of gently stirring, the solution was filtered and the absorbance at 328 nm of the filtered solution was measured. Experiments were performed in duplicate. A linear calibration curve was constructed using methanolic solutions of the extract. From supernatant average absorption value, the mass of the non-encapsulated PExt was calculated and applied in Eq 2:

$$EE(\%) = \frac{\text{Total mass of compound} - (\text{non} - \text{encapsulated compound mass})}{\text{Total mass of compound}} x100 \quad (2)$$

## Preparation of PLA and PLA-$NP_{PEXT}$ films

PLA films were obtained via the solution-casting method as follows: 1 g of commercial high molecular weight PLA, previously purified as described before, was added to 11 mL of dichloromethane (DCM) and the mixture was stirred for 1 hour at room temperature. Thereafter, the PLA solution was cast on glass petri dishes, dried under ambient condition for 24 h and further oven dried under vacuum at 50 °C for 24 h.

In the case of PLA-$NP_{PEXT}$ films, 12.2 mg of lyophilized $NP_{PExt}$ were sonicated for 1 min in 2 mL of DCM prior to adding to the DMC PLA solution, prepared as described above. Then, the mixture was cast on glass petri dishes and dried in the conditions described above.

## Particle size and polydispersity index

Nanoparticle size was measured by using dynamic light scattering (DLS) (Zetasizer Nano-ZS of Malvern Instruments). Prior to analyses, nanoparticle suspension (100 μl) was diluted in 900 μl of deionized water. For each sample, both the particle size (PS) and the polydispersity index (PdI) were calculated in triplicate, at 25 ± 1 °C at a scattering angle of 173°.

## Tensile tests

Uniaxial tensile tests were carried out on type IV (ASTM D638) dumbbell samples cut out from the PLA matrix and nanocomposite films using an INSTRON dynamometer 5982 with a crosshead speed of 5 mm / min and using a load cell of 1 kN . Stress-strain curves were obtained from these tests, and tensile parameters (Young's modulus, tensile strength, and strain at break) were determined from the curves. The measurements were performed at room temperature and at least five samples for each material were tested. Average values and their deviations are reported.

### Scanning electron microscopy (SEM)

Nanoparticles or films (cryogenically fractured) were deposited on microscope glasses and vacuum dried at 50°C for 24 h. Samples were coated with gold using an ion sputter coater and observed by using a scanning electron microscope Zeiss Supra 40 with field emission gun operated at 3 kV. Images were processed by using digital image analysis software (ImageJ).

### Transmission electron microscopy (TEM)

Transmission electron micrographs of PLA nanoparticles were taken with an EM 301 Philips transmission electron microscope at an acceleration voltage of 60 kV. A drop of the nanoparticle suspension was deposited onto a carbon coated microscopy grid and negatively stained with an aqueous 2% solution of uranyl acetate for 1 min. The liquid in excess was blotted with filter paper and the remaining liquid was dried before the specimen observation.

### Migration studies

To study the release of the antioxidant-loaded nanoparticles from the PLA films, samples of 100 $mm^2$ were immersed in 100 mL of distillate water and kept at room temperature, under magnetic stirring. Samples were taken at different times, i.e. 2, 5, 10, 20 and 30 days of incubation in order to follow the release by UV-Vis spectrometry and observed by SEM.

### Thermal analysis

Thermogravimetric analyses were carried out using a TGA-60 Shimadzu thermogravimetric analyzer under $N_2$ atmosphere. Samples (5-7 mg) were placed into alumina crucibles and heated from room temperature to 500°C at a heating rate of 10 °C $min^{-1}$.

Differential scanning calorimetry (DSC) measurements were made on a TA Q20 differential scanning calorimeter under dry nitrogen atmosphere. Indium standard was used for calibration. Dynamic experiments were performed to obtain Tg values of nanostructured thermosets. Films were first removed from the substrate and placed (5−10 mg) in the DSC pan. Samples were heated to 200 °C, and the temperature was held for 10 min to remove the thermal history. Subsequently, the samples were cooled to −70 °C for 15 min and heated to 200 °C at a rate of 5 °C $min^{-1}$. All Tg values were taken as the midpoint of the transition during the second heating scan.

## Results and discussion

### Phenolic acid composition of PExt

Phenolic acids detected in major proportion were: chlorogenic (CLA); caffeic; 4,5- dicaffeoylquinic (4,5-DCQ); 3,5-dicaffeoylquinic (3,5-DCQ); 3,4-dicaffeoylquinic (3,4-DCQ) and chlorogenic acid, being 4,5 DCQ and CLA the most abundant (HPLC chromatogram of phenolic acids is presented in supplementary data). On the other hand, caffeic acid was the phenolic structure found in minor proportion. A high proportion of 3,5-DCQ and CLA acids in the tissue of purple-skinned sweet potatoes has already been reported for other plant varieties (Beauregard, Evangeline, Golden Sweet).[27, 28] Figure 1 shows the chemical structure of the phenolic acid found in the sweet potato extract and their content (expressed in mg $kg^{-1}$ of fresh peel weight).

The concentration of chlorogenic acid found in this extract (784 mg $kg^{-1}$ fresh weight), was considerably higher than that observed in other varieties of this root (usually ranging from 117 to 467 mg $kg^{-1}$ fresh weight) [29]. Many studies have linked chlorogenic acid consumption to a wide range of health benefits, including neuroprotection, cardioprotection, weight loss, chemopreventive properties, anti-inflammatory activity, decreased blood pressure, decreased diet-induced insulin resistance, decreased blood pressure, anxiolytic effects, and antihyperalgesic effects. Pre-clinical and clinical studies provide evidence that chlorogenic acid supplementation could protect against neurological degeneration and resulting diseases associated with oxidative stress in the brain [30–33].

Considering the multiple benefits associated with consumption in the diet of chlorogenic acid, the possibility of obtaining it from vegetal waste makes this methodology attractive from the point of view of health and cost-effectiveness.

### Antioxidant activity

From the DPPH radical inhibition assay (see supplementary data), the calculated IC50 of the PExt was equivalent to 476.96 mg of TROLOX $mL^{-1}$. The TEAC of the extract is even more relevant when comparing with values obtained for other vegetal sources such as orange juice (6.64 mg TROLOX $mL^{-1}$) or limonene (1.26 mg TROLOX $mL^{-1}$)[24, 25].

These values show that the effect of this antioxidant is more significant than most other species, giving great added value to the sweet potato peel, which is considered as a waste in the potato industry.





Journal : Large 10965 | Article No : 2346 | Pages : 12 | MS Code : 2346 | Dispatch : 13-11-2020

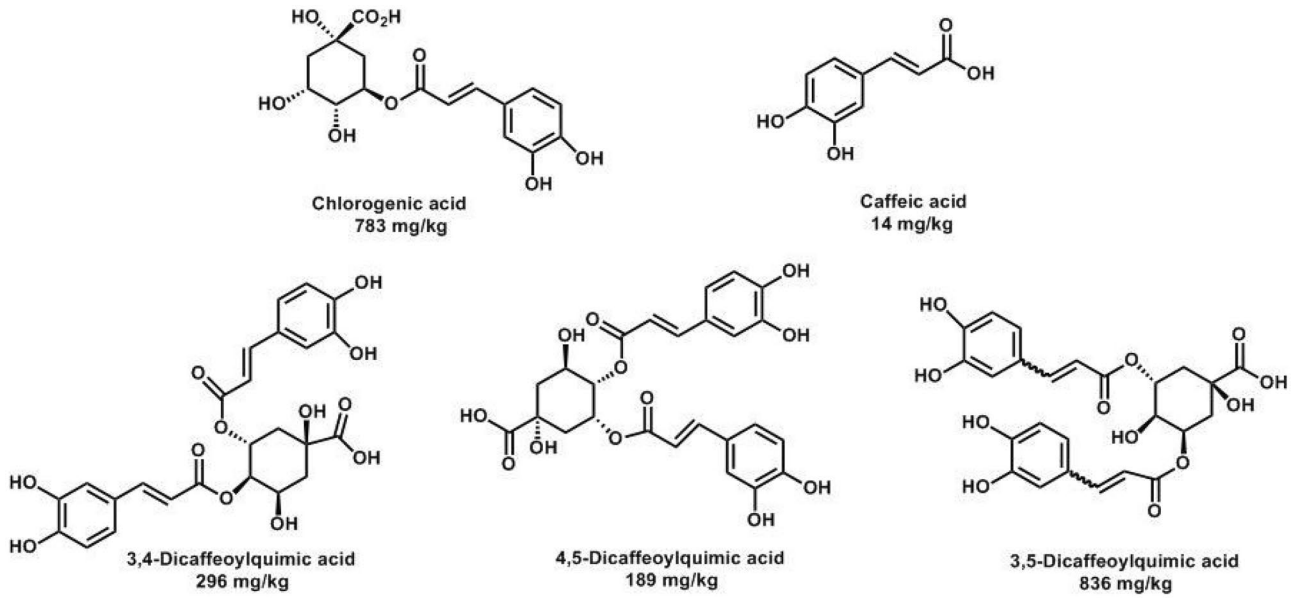


**Fig. 1** Phenolic acids found in the sweet potato peel extract (content is expressed in mg $kg^{-1}$ of fresh peel weight)

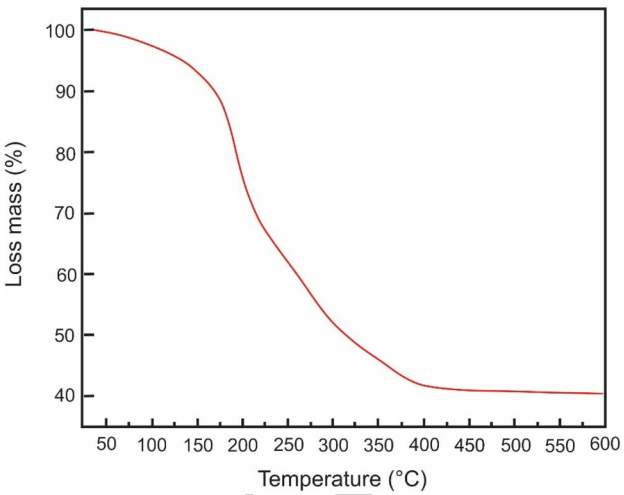


**Fig. 2** Thermogravimetric analysis of PExt

## Thermogravimetric analysis (TGA)

In the thermogram for the extract of the sweet potato skin (Fig. 2) a first mass loss (4.5%) was observed between 30 and 135 °C, attributed to the loss of water and volatile low molecular weight compounds.[27]. From 135 °C to approximately 170 °C, a weight loss of 5.5% was observed, attributed to the degradation of volatile compounds, polar lipids, and small acid molecules. At higher temperatures, the weight mass loss was due to pyrolysis of compounds such as insoluble fiber: cellulose, hemicellulose and lignin. [34]. The residue was approximately 43%.

It is important to note that, since degradation of the extract starts at a higher temperature (135 ° C) than temperature used in encapsulation protocol, then the extract properties should not have been affected during the encapsulation process.

## Characterization of NP by SEM and DLS

PLA nanoparticles were characterized by scanning electron microscopy (SEM) and dynamic light scattering (DLS). The best results were achieved when the nanoparticles where synthesized using PLA with a molecular weight of 24,500 g $mol^{-1}$ under an RCF of 10733, and for 20 min. SEM micrographs showed nanoparticles with spherical morphology, regular surface and homogeneous size (Fig. 3a and 3b) with an average size of 74 nm (Fig. 3c). On the other hand, and as expected, the average hydrodynamic diameter (Dh) measured by DLS was slightly higher than that measured by SEM (121 nm), because in the DLS technique, NPs are solvated. The polydispersity index (PdI) was 0.13.

On the contrary, when the synthesis was carried out using lower molecular weight PLA (18,000 g $mol^{-1}$) and shorter centrifugation times (40 min), the presence of surfactant surrounding the nanoparticles was observed in the images. A summary of the parameters evaluated for each method (SEM and DLS) is shown in supporting.



Journal : Large 10965 | Article No : 2346 | Pages : 12 | MS Code : 2346 | Dispatch : 13-11-2020

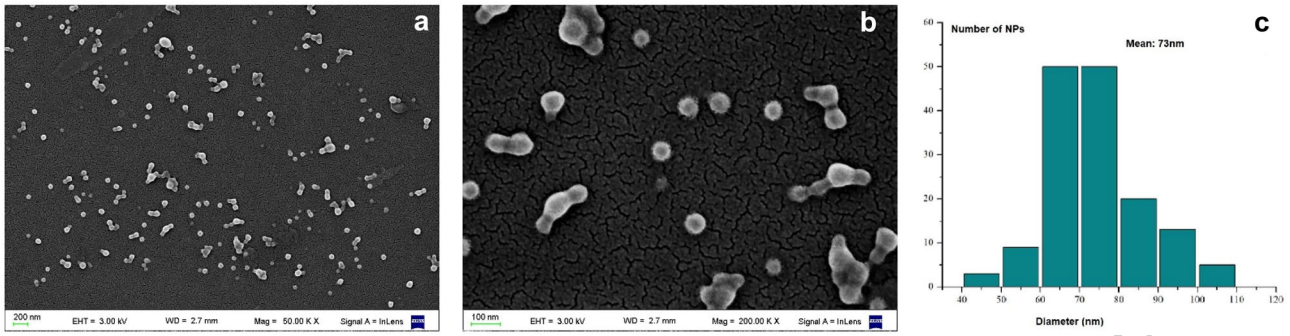


**Fig. 3** **a** and **b** SEM micrographs (50 K X and 200K X), of the nanoparticles (centrifugation time 20 min, PLA Mw: 24, 500 g mol $^{-1}$) **c** Nanoparticles size distribution

## Evaluation of encapsulation through the encapsulation efficiency, size, and morphology of particles with different variables

### Influence of solvents on the nanoparticle's synthesis

In the emulsification-evaporation method, an internal organic phase (polymer and extract) is added to an external phase that contains the surfactant or stabilizer (in our case (PVA + Water, aqueous phase), which is evaporated to obtain the nanoparticles. The success in the formation of the nanoparticles depends on the degree of emulsification achieved by mixing the internal and external phases in the process, so a search for the right solvent is required. For the internal phase, different solvent systems were evaluated:

System 1: PLA / Extract: Acetone / Water

System 2: PLA / Extract: Acetone: Water 3: 1 / Acetone: Water 3: 1

System 3: PLA / Extract: Acetone / Methanol

The best results were obtained when the nanoparticles were synthesized using as internal with PLA in acetone and the pellet was resuspended in methanol (solvent system 3). In this condition, SEM micrographs showed nanoparticles with spherical morphology and regular surface (Figs. 4a and 4b) with an average size of 84 nm (Fig. 4c), throughout the entire sample. The results observed for the other solvent systems can be found in supplementary data.

Figure 5 shows a TEM micrograph of PLA nanoparticles. TEM was made using a drop of a suspension of the nanoparticles. As can be seen, nanoparticles have an average size of 80 nm and form aggregates of 1 mm. The encapsulation efficiency was 96 %. The use of methanol as a solvent avoids the formation of agglomerates, probably due to its low affinity with PLA, allowing a better organization of the polymer chains. The viscosity of methanol (0.59 cp. at 20 °C) could also prevent the aggregation through an efficient stabilization of the nanoparticles[35]. Besides, the high encapsulation efficiency achieved using the methanolic antioxidant extract suggests that methanol could also prevent the migration of the antioxidant into the aqueous phase.



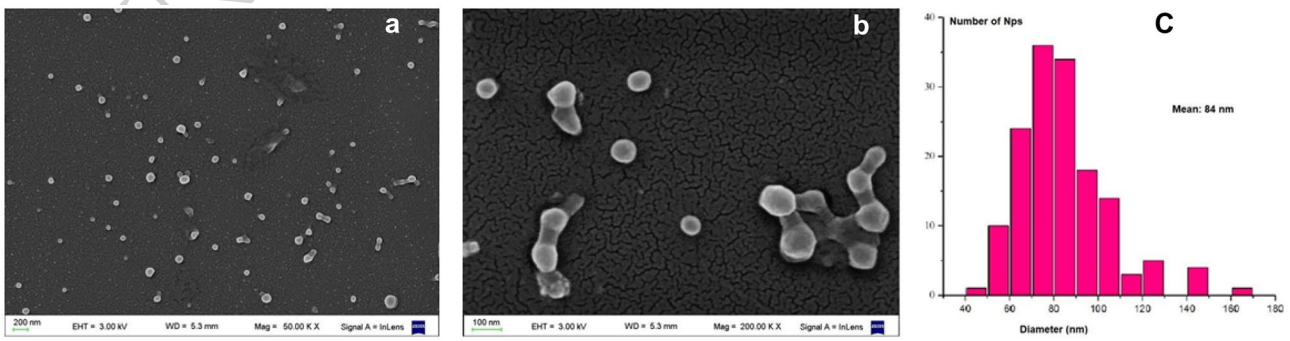


**Fig. 4** **a** and **b** SEM micrographs (50K X and 200K X), of the nanoparticles prepared using the solvent system 3 (PLA/ acetone: PExt/methanol) **c** Nanoparticles size distribution calculated from the SEM images



Journal : Large 10965 | Article No : 2346 | Pages : 12 | MS Code : 2346 | Dispatch : 13-11-2020

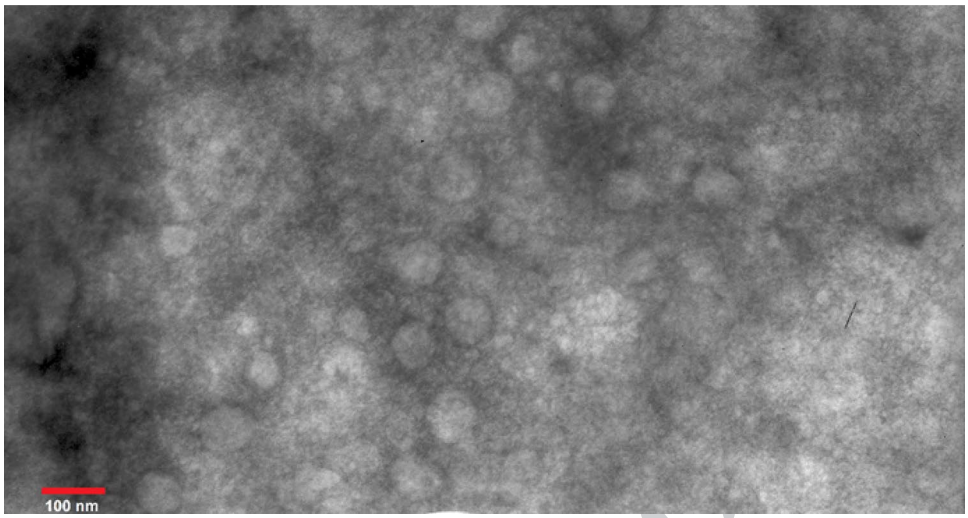


**Fig. 5** TEM micrographs of the nanoparticles (centrifugation time 20 min, PLA Mw: 24, 500 g mol $^{-1}$)

## Influence of the PExt: PLA ratio, centrifugation parameters and PLA molecular weight

The influence of different parameters in the encapsulation efficiency was evaluated: PExt: PLA ratio (0.2-0.6), centrifugation time (20-40 min), RCF (10733 or 18138) and PLA molecular weight ($M_W$= 18,000 or 24,500 g mol$^{-1}$).

In summary, longer times, lower PLA molecular weight and low temperatures favor the formation of aggregates (Summary in supplementary data). The best encapsulation efficiency (96%) was observed for the following conditions: PExt: PLA ratio: 0.2; Centrifugation time: 20 min; RCF of 10733; PLA molecular weight 24,500 g mol$^{-1}$

## Thermal analysis by differential scanning calorimetry (DSC)

Figure 6 shows DSC traces for PLA (low molecular weight), NP, and nanoparticles with PLA:PExt ratios of 0.2 and 0.6. From this figure, we can observe that all the samples exhibit a transition at 55 °C attributed to the glass transition. It shows that the hydrodynamic volume for all samples does not vary greatly between them. A similar phenomenon was described for other PLA films containing nanoparticles [20, 36].

On the other hand, PLA exhibit a cold crystallization peak near 100 °C [20, 37, 38]. For loaded nanoparticles this peak shift to higher temperatures according to the antioxidant content. The occurrence of cold crystallization is due to the heating rate (5 °C/min in our case) which is slow enough to allow smaller PLA crystals to melt and recrystallize[39].

The melting of PLA occurred around 130-140 °C as shown by an endothermic peak, possibly resulting from the superposition of two peaks. Yuzay et al.[40] reported this fact as a consequence of formation of a disordered alpha phase, existence of more than one crystalline structure and different morphologies formed during the heating and cooling process[37]. In the case of NPs, were observed two glass transition temperature (Tg) defining the different crystalline structures that appear superposed in PLA pellets. Also, two narrow endothermic peaks have been observed at 145 °C and 151 °C.

The crystallinity results are generally different to that which occurs at a nanoscale and this occurs mainly because of the ratio of surface atoms to the total atoms in the material. This effect is observed between the PLA pellets and the nanoscale PLA in different reports [41–43].

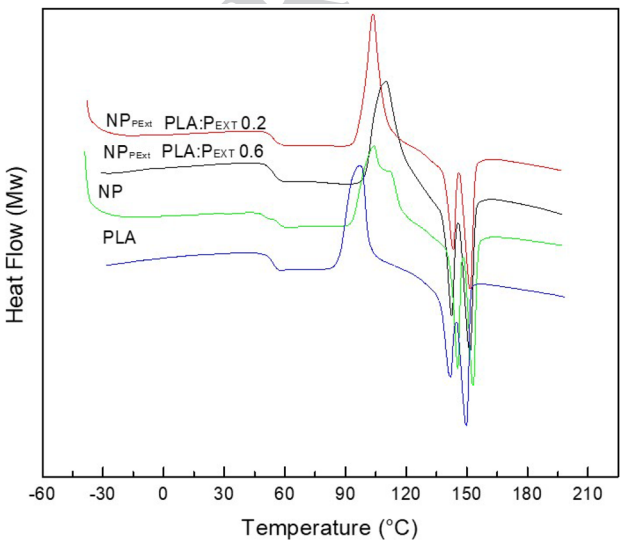


**Fig. 6** DSC thermograms for PLA, NPLA and $NP_{PExt}$ at differents PLA:PExt ratios





Journal : Large 10965 | Article No : 2346 | Pages : 12 | MS Code : 2346 | Dispatch : 13-11-2020

## Mechanical properties

The mechanical properties of the films are reported in Table 1 and the representative stress–strain curves for the samples are shown in Fig. 7 for neat PLA, PLA with nanoparticles loaded with extract ($NP_{PExt}$) and PLA films loaded with $NP_{PExt}$ after 30 days after beginning the migration experiments.

The results show that the addition of nanoparticles had an effect on the mechanical properties of the PLA film. As seen in Table 1, the elongation at break as well as the work of fracture increased, while the tensile modulus and the tensile strength decreased. The addition of NP with ratio PLA:PExt of 0.2 raised the elongation at break by 171% % and the work of fracture by 47%.

Other studies have also shown an increase in the elongation at break with the addition of nanoparticles; for example, Jiang et al.[44] reported that the elongation at break of PLA increased by 33% with the addition of 5 wt% and 7.5 wt% of $CaCO_3$ nanoparticles and increased by 433% with the addition of 2.5 wt% of montmorillonite nanoparticles. The solvent (used in the preparation of the films) remains in the polymer network and has a positive effect on the elongation at break and other ductile properties, since it acts as a plasticizer[45]. Probably the nanoparticles influence the entrapment and dispersion of the solvent, which remains in the intramolecular network despite the drying stage of the films. It is very likely that the nanoparticles generate a tortuous path[46] and hinder the passage of the solvent and this is reflected in this plasticizing effect different from that observed for neat PLA.

However, when the film was tested after 30 days of release, although the young's modulus was maintained and the elongation at break remained close to the value of the PLA film, the value of the tensile strength was reduced by almost 50% and the work of fracture by 72%. These results show that that both the film and the nanoparticles possibly present quite different characteristics to the initial ones, propitiated by the particular process of antioxidant release, which directly impact the mechanical properties. This will be further corroborated by observing the morphology of the films by SEM.

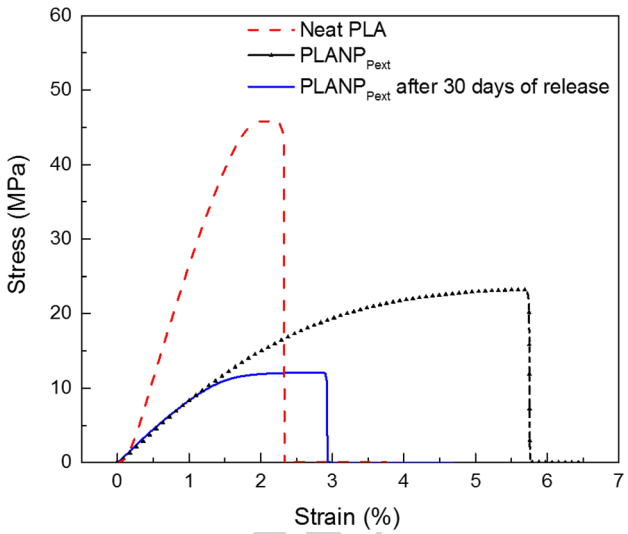


**Fig. 7** Stress-Strain curves for PLA, $PLANP_{PExt}$ and $PLANP_{PExt}$ after 30 days of release

## Morphology of films

SEM micrographs of the fractured surfaces of PLA (molecular weight 200,000 g $mol^{-1}$) and its nanocomposites $PLANP_{PExt}$ are shown in Fig. 8.

The fractured surface for the PLA film showed a typical brittle fracture (Fig. 7c) as expected and in agreement with tensile test results, where neat PLA exhibited an elongation at break of only 2%. When comparing the morphology of the neat PLA film to that of the nanocomposite (Figs. 7b and 7d) it clearly appears that the fractured surface for the nanocomposite is shows numerous crazes, indicating a massive crazing effect which resulted in a ductile fracture[46]. This is in accordance with the effect that was noticed from tensile tests with an elongation at break of 6% (Table 1).

This type of fractured surface is also observed when the solvent acts as a plasticizer, as discussed in the mechanical properties section. The dispersed nanoparticles most likely influence the entrapment of the solvent. On the other hand, no phase separation was observed, as expected considering the structural similarity between the matrix (high molecular weight PLA) and the shell of the nanoparticles (low molecular weight PLA).

**Table 1** Mechanical properties for PLA, $PLANP_{PExt}$ and $PLANP_{PExt}$ after 30 days of migration studies

| Film | Tensile Strength (MPa) | Tensile Modulus (GPa) | Elongation at Break (%) | Work of Fracture (MPa) |
|---|---|---|---|---|
| Neat PLA | 45.3 ± 3.1 | 3.1 ± 0.4 | 2.3 ± 0.5 | 0.6 ± 0.2 |
| $PLANP_{PExt}$ (PLA/PExt: 0.2) | 23.1 ± 1.0 | 0.8 ± 0.2 | 6.0 ± 0.1 | 0.9 ± 0.1 |
| PLA-$NP_{PExt}$ after 30 days | 12.0 ± 0.8 | 0.9 ± 0.1 | 3.0 ± 0.1 | 0.3 ± 0.1 |





Journal : Large 10965 | Article No : 2346 | Pages : 12 | MS Code : 2346 | Dispatch : 13-11-2020

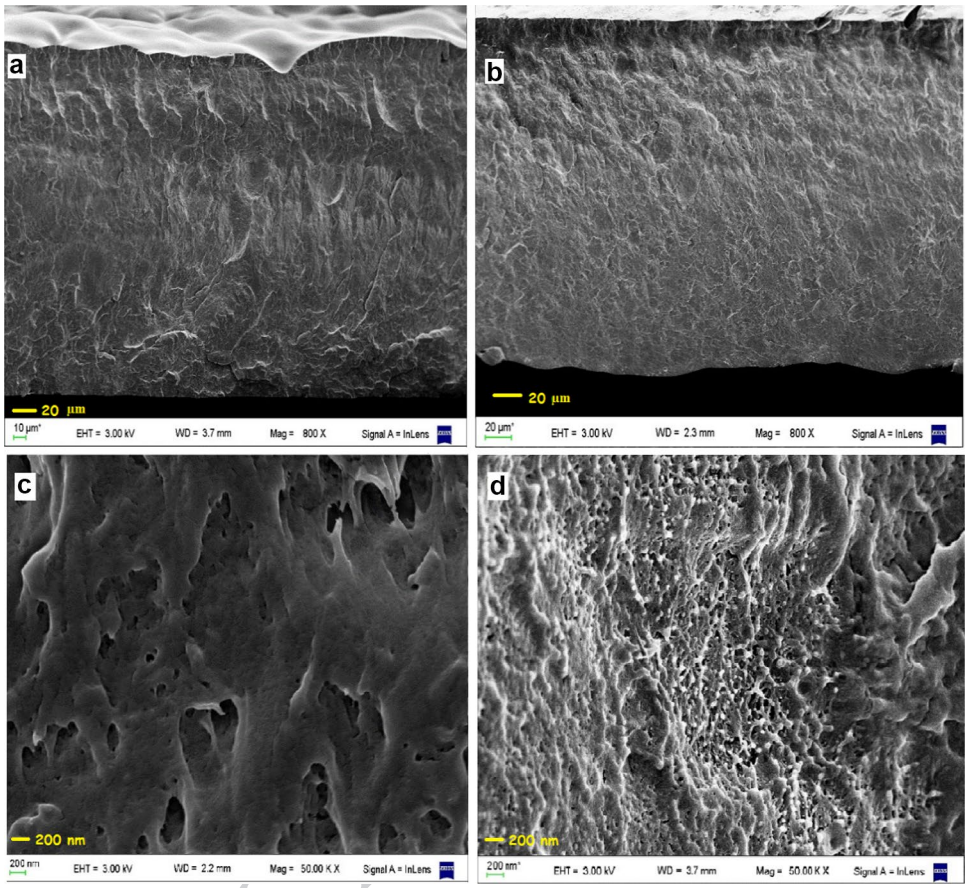


**Fig. 8** SEM Micrographs of the fractured surface for PLA (**a** and **c**) and PLA with $NP_{PExt}$ (**b** and **d**)

## Migration study by SEM

Specific migration tests of PExt from the film was studied in simulant distilled water and performed according to European Standard EN 13130 Part 1 (European Standard 2004).

Samples taken at different times were analyzed by UV spectroscopy. The measurements recorded before 30 days of release showed absorbances corresponding to very low concentrations of the antioxidant, with values close to the equipment error. After 30 days of testing, the absorbance recorded corresponds to less than 5% of the amount of added extract, suggesting that the release of it is very slow from the film. Since the detection of migration by UV is almost imperceptible, we decided to evaluate how the release affects the surface of the film, during the same time of migration study by SEM.

SEM micrographs of PLA films loaded with $NP_{PExt}$ (PLA: PExt ratio 0.2) were taken at different times during the release experiment. The sequence of images is displayed in Fig. 9.

The image taken 30 days after the beginning of the study (Fig. 9b) showed the total disappearance of the nanoparticles and empty holes (yellow arrow) where the nanoparticles were inserted before the release study.

It is important to note that, during the study, the nanoparticles observed in the fractured surfaces have been deformed and gradually released to the medium in which the film was immersed as shown in Fig. 10.

This type of morphology supports the values obtained for the mechanical properties, since although the elongation at break decreased by 50%, most likely due to the presence of holes that are observed in Fig. 8, the values of the modulus and tensile strength indicate that there is still some plasticization given by the process of migration of the antioxidant. The value of the modulus does not vary considerably, indicating the presence of some nanoparticles in the process of deformation, as shown in Fig. 9.

## Conclusions

In this work, nanoparticles of uniform size and shape loaded with natural antioxidants were successfully synthesized. Low molecular weight polylactic acid-coated particles were uniformly dispersed in films prepared with high molecular weight PLA, from which the complete release of the nanoparticles was observed one month after being exposed to an aqueous medium. But the main achievement of this work is the fact that the antioxidants were obtained from a vegetable

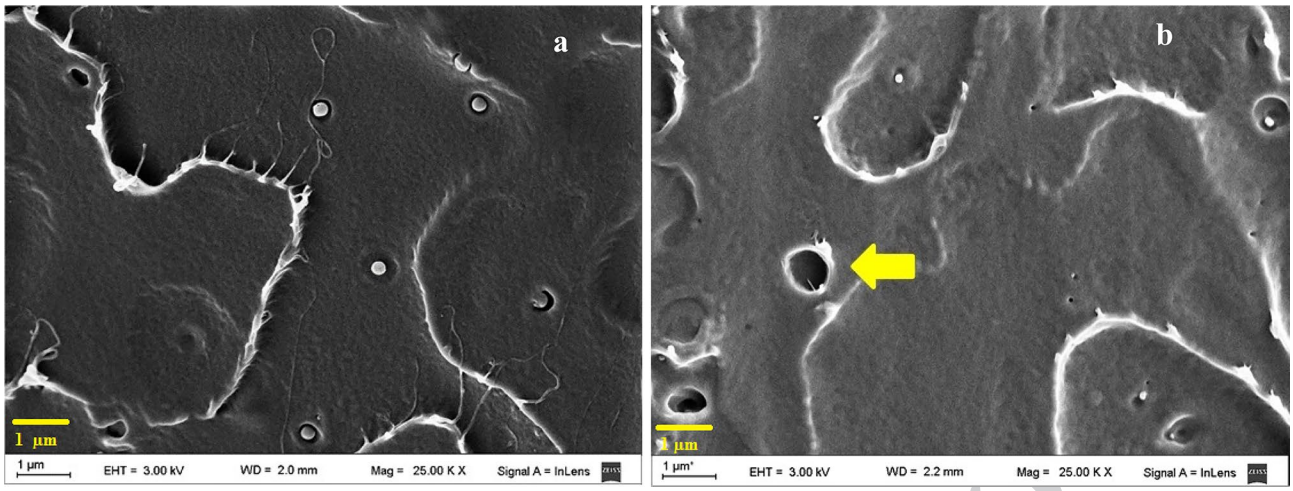


**Fig. 9** SEM Micrographs **a** Image taken at the beginning of the release experiment; **b** Image taken 30 days after the beginning of the study

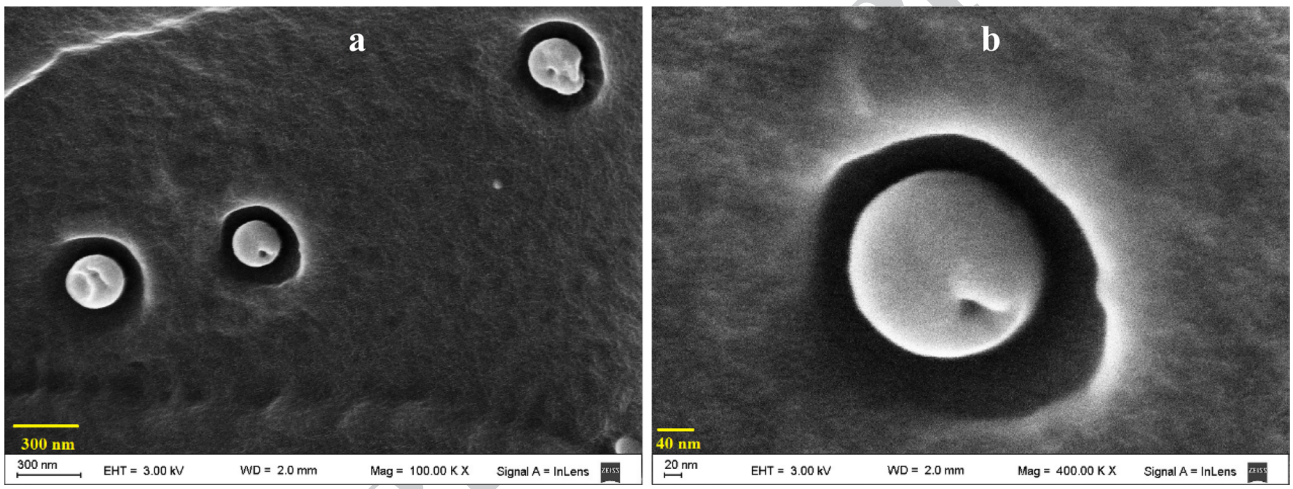


**Fig. 10** SEM Micrographs of $NP_{PExt}$. Images taken 72 hours after starting the release study. **a** 100K X and **b** 400K X)

waste which is beneficial from both an economic and an environmental point of view. Besides, the thermal stability of the nanocapsules opens the possibility of incorporating them in different polymer matrices, even in those obtained through an extrusion process.

From the results presented in this article, the new biodegradable nanoparticles can be proposed to be incorporated into films with antioxidant properties that extend the preservation times of the products they cover.

**Acknowledgements** The authors thank the financial supportof UBACyT (No. 20020130100021BA), ANPCyT, (PICT- 2012-0717) and CONICET (PIP 2013– 11220110100370CO). Authors acknowledge the skillful contributions for use of HPLC to Professor Dr. Marina Ciancia of Facultad de Agronomía, Departamento de Biología Aplicada y Alimentos, Universidad de Buenos Aires, Argentina and Dr. Celina Bernal of Facultad de Ingenieria, Universidad de Buenos Aires. LGP2 is part of the LabEx Tec 21 (Investissements d'Avenir - grant agreement n°ANR-11-LABX-0030) and of the PolyNat Carnot Institut (Investissements d'Avenir - grant agreement n°ANR-11-CARN-030-01).

## References

1. Kaczmarek B, Sionkowska A, Kozlowska J, Osyczka AM (2018) New composite materials prepared by calcium phosphate precipitation in chitosan/collagen/hyaluronic acid sponge cross-linked by EDC/NHS. Int J Biol Macromol 107:247–253. https://doi.org/10.1016/J.IJBIOMAC.2017.08.173
2. Restuccia D, Spizzirri UG, Parisi OI et al (2010) New EU regulation aspects and global market of active and intelligent packaging for food industry applications. Food Control 21:1425–1435. https://doi.org/10.1016/j.foodcont.2010.04.028
3. Fang Z, Zhao Y, Warner RD, Johnson SK (2017) Active and intelligent packaging in meat industry. Trends Food Sci Technol 61:60–71. https://doi.org/10.1016/j.tifs.2017.01.002
4. Yang S, Bai S, Wang Q (2018) Sustainable packaging biocomposites from polylactic acid and wheat straw: Enhanced physical



Journal : Large 10965 | Article No : 2346 | Pages : 12 | MS Code : 2346 | Dispatch : 13-11-2020

performance by solid state shear milling process. Compos Sci Technol 158:34–42. https://doi.org/10.1016/j.compscitech.2017.12.026
5. Beckman CH (2000) Phenolic-storing cells: Keys to programmed cell death and periderm formation in wilt disease resistance and in general defence responses in plants? Physiol Mol Plant Pathol 57:101–110. https://doi.org/10.1006/pmpp.2000.0287
6. Ballesteros LF, Ramirez MJ, Orrego CE et al (2017) Encapsulation of antioxidant phenolic compounds extracted from spent coffee grounds by freeze-drying and spray-drying using different coating materials. Food Chem 237:623–631. https://doi.org/10.1016/j.foodchem.2017.05.142
7. Rostami M, Yousefi M, Khezerlou A et al (2019) Application of different biopolymers for nanoencapsulation of antioxidants via electrohydrodynamic processes. Food Hydrocoll 97:105170. https://doi.org/10.1016/J.FOODHYD.2019.06.015
8. Ghasemi S, Jafari SM, Assadpour E, Khomeiri M (2018) Nanoencapsulation of d-limonene within nanocarriers produced by pectin-whey protein complexes. Food Hydrocoll 77:152–162. https://doi.org/10.1016/J.FOODHYD.2017.09.030
9. Zhao Y, Sun W, Saldaña MDA (2018) Nanogels of poly-N-isopropylacrylamide, poly-N, N-diethylacrylamide and acrylic acid for controlled release of thymol. J Polym Res 25. https://doi.org/10.1007/s10965-018-1644-x
10. Torkamani AE, Syahariza ZA, Norziah MH et al (2018) Encapsulation of polyphenolic antioxidants obtained from Momordica charantia fruit within zein/gelatin shell core fibers via coaxial electrospinning. Food Biosci 21:60–71. https://doi.org/10.1016/J.FBIO.2017.12.001
11. Gandía-Herrero F, Cabanes J, Escribano J et al (2013) Encapsulation of the Most Potent Antioxidant Betalains in Edible Matrixes as Powders of Different Colors. J Agric Food Chem 61:4294–4302. https://doi.org/10.1021/jf400337g
12. Huang X, Dai Y, Cai J et al (2017) Resveratrol encapsulation in core-shell biopolymer nanoparticles: Impact on antioxidant and anticancer activities. Food Hydrocoll 64:157–165. https://doi.org/10.1016/J.FOODHYD.2016.10.029
13. Cuq B, Gontard N, Aymard C, Guilbert S (1997) Relative humidity and temperature effects on mechanical and water vapor barrier properties of myofibrillar protein-based films. Polym Gels Networks 5:1–15. https://doi.org/10.1016/S0966-7822(96)00026-3
14. Aytac Z, Kusku SI, Durgun E, Uyar T (2016) Encapsulation of gallic acid/cyclodextrin inclusion complex in electrospun polylactic acid nanofibers: Release behavior and antioxidant activity of gallic acid. Mater Sci Eng C 63:231–239. https://doi.org/10.1016/J.MSEC.2016.02.063
15. Huang X, Liu Y, Zou Y et al (2019) Encapsulation of resveratrol in zein/pectin core-shell nanoparticles: Stability, bioaccessibility, and antioxidant capacity after simulated gastrointestinal digestion. Food Hydrocoll 93:261–269. https://doi.org/10.1016/J.FOODHYD.2019.02.039
16. de Meneses AC, dos Santos PCM, Machado TO, et al (2017) Poly(thioether-ester) nanoparticles entrapping clove oil for antioxidant activity improvement. J Polym Res 24:. https://doi.org/10.1007/s10965-017-1353-x
17. Lee CH, Nalluri LP, Popuri SR (2019) Optimization studies for encapsulation and controlled release of curcumin drug using Zn+2 cross-linked alginate and carboxy methylcellulose blend. J Polym Res 26:. https://doi.org/10.1007/s10965-018-1667-3
18. Pan F, Chen L, Jiang Y et al (2018) Bio-based UV protective films prepared with polylactic acid (PLA) and Phoebe zhennan extractives. Int J Biol Macromol 119:582–587. https://doi.org/10.1016/J.IJBIOMAC.2018.07.189
19. Krishnan S, Mohanty S, Nayak SK (2018) An eco-friendly approach for toughening of polylactic acid from itaconic acid based elastomer. J Polym Res 25:. https://doi.org/10.1007/s10965-017-1421-2
20. Pantani R, Gorrasi G, Vigliotta G et al (2013) PLA-ZnO nanocomposite films: Water vapor barrier properties and specific end-use characteristics. Eur Polym J 49:3471–3482. https://doi.org/10.1016/j.eurpolymj.2013.08.005
21. Ng HM, Bee ST, Sin LT et al (2020) Interaction Effect of Scomberomorus Guttatus-Derived Hydroxyapatite and Montmorillonite on the Characteristics of Polylactic Acid Blends for Biomedical Application. J Polym Res 27. https://doi.org/10.1007/s10965-020-02138-w
22. Zhang W, Wang Y (2008) Synthesis and Properties of High Molecular Weight. Chinese J Polym Sci 26:425–432. https://doi.org/10.1246/nikkashi1898.72.4_1018
23. Brand-Williams W, Cuvelier MEE, Berset C (1995) Use of a free radical method to evaluate antioxidant activity. Leb u- Technol 28:25–30. https://doi.org/10.1016/S0023-6438(95)80008-5
24. Bacanli M, Başaran AA, Başaran N (2015) The antioxidant and antigenotoxic properties of citrus phenolics limonene and naringin. Food Chem Toxicol 81:160–170. https://doi.org/10.1016/j.fct.2015.04.015
25. Wang H, Cao G, Prior RL (1996) Total antioxidant capacity of fruits. J Agric Food Chem 44:701–705. https://doi.org/10.1021/jf950579y
26. Roussaki M, Gaitanarou A, Diamanti PC et al (2014) Encapsulation of the natural antioxidant aureusidin in biodegradable PLA nanoparticles. Polym Degrad Stab 108:182–187. https://doi.org/10.1016/j.polymdegradstab.2014.08.004
27. Padda MS, Picha DH (2008) Quantification of phenolic acids and antioxidant activity in sweetpotato genotypes. Sci Hortic (Amsterdam) 119:17–20. https://doi.org/10.1016/j.scienta.2008.07.008
28. Jung J, Lee S, Kozukue N et al (2011) Journal of Food Composition and Analysis Distribution of phenolic compounds and antioxidative activities in parts of sweet potato ( Ipomoea batata L.) plants and in home processed roots. J Food Compos Anal 24:29–37. https://doi.org/10.1016/j.jfca.2010.03.025
29. Shahidi, F., & Naczk M (2003) Shahidi, F., & Naczk, M. (2003). . In F. Shahidi, & M. Naczk, Phenolics in Food and Nutraceuticals (p. 576). CRC Press. In: Food and NutraceuticalsPhenolics. CRC Press, p 576
30. Wen S, Liang M, Zou R et al (2015) Electrospinning of palladium/silica nanofibers for catalyst applications. RSC Adv 5:41513–41519. https://doi.org/10.1039/C5RA02660A
31. Zhang Y, Liu W, Liu C et al (2014) Retrogradation behaviour of high-amylose rice starch prepared by improved extrusion cooking technology. Food Chem 158:255–261. https://doi.org/10.1016/j.foodchem.2014.02.072
32. Olthof MR, Hollman PCH, Katan MB (2001) Chlorogenic Acid and Caffeic Acid Are Absorbed in Humans. J Nutr 131:66–71. https://doi.org/10.1093/jn/131.1.66
33. Belkaid A, Currie JC, Desgagnés J, Annabi B (2006) The chemopreventive properties of chlorogenic acid reveal a potential new role for the microsomal glucose-6-phosphate translocase in brain tumor progression. Cancer Cell Int 6. https://doi.org/10.1186/1475-2867-6-7
34. Wang T, Dong X, Jin Z et al (2015) Pyrolytic characteristics of sweet potato vine. Bioresour Technol 192:799–801. https://doi.org/10.1016/j.biortech.2015.05.018
35. Peltonen L, Koistinen P, Karjalainen M et al (2002) The effect of cosolvents on the formulation of nanoparticles from low-molecular-weight poly(l)lactide. AAPS PharmSciTech 3:E32. https://doi.org/10.1208/pt030432
36. Nonato RC, Mei LHI, Bonse BC et al (2019) Nanocomposites of PLA containing ZnO nanofibers made by solvent cast 3D printing: Production and characterization. Eur Polym J 114:271–278. https://doi.org/10.1016/J.EURPOLYMJ.2019.02.026

37. Bussière P-O, Peyroux J, Chadeyron G, Therias S (2013) Influence of functional nanoparticles on the photostability of polymer materials: Recent progress and further applications. Polym Degrad Stab 98:2411–2418. https://doi.org/10.1016/J.POLYMDEGRADSTAB.2013.06.009
38. Xu C, Yuan D, Fu L, Chen Y (2014) Physical blend of PLA/NR with co-continuous phase structure: Preparation, rheology property, mechanical properties and morphology. Polym Test 37:94–101. https://doi.org/10.1016/J.POLYMERTESTING.2014.05.005
39. Du Y, Wu T, Yan N et al (2014) Fabrication and characterization of fully biodegradable natural fiber-reinforced poly(lactic acid) composites. Compos Part B Eng 56:717–723. https://doi.org/10.1016/J.COMPOSITESB.2013.09.012
40. Yuzay IE, Auras R, Soto-Valdez H, Selke S (2010) Effects of synthetic and natural zeolites on morphology and thermal degradation of poly(lactic acid) composites. Polym Degrad Stab 95:1769–1777. https://doi.org/10.1016/J.POLYMDEGRADSTAB.2010.05.011
41. Wrona M, Cran MJ, Nerín C, Bigger SW (2017) Development and characterisation of HPMC films containing PLA nanoparticles loaded with green tea extract for food packaging applications. Carbohydr Polym 156. https://doi.org/10.1016/j.carbpol.2016.08.094
42. Gupta SK, Talati M, Jha PK (2008) Shape and size dependent melting point temperature of nanoparticles. In: Materials Science Forum
43. Kim EH, Lee BJ (2009) Size dependency of melting point of crystalline nano particles and nano wires: A thermodynamic modeling. Met Mater Int 15. https://doi.org/10.1007/s12540-009-0531-8
44. Jiang L, Zhang J, Wolcott MP (2007) Comparison of polylactide/nano-sized calcium carbonate and polylactide/montmorillonite composites: Reinforcing effects and toughening mechanisms. Polymer (Guildf) 48:7632–7644. https://doi.org/10.1016/J.POLYMER.2007.11.001
45. Mele G, Bloise E, Cosentino F et al (2019) Influence of Cardanol Oil on the Properties of Poly(lactic acid) Films Produced by Melt Extrusion. ACS Omega 4:718–726. https://doi.org/10.1021/acsomega.8b02880
46. Herrera N, Mathew AP, Oksman K (2015) Plasticized polylactic acid/cellulose nanocomposites prepared using melt-extrusion and liquid feeding: Mechanical, thermal and optical properties. Compos Sci Technol 106:149–155. https://doi.org/10.1016/j.compscitech.2014.11.012







| Journal : Large 10965 | Article No : 2346 | Pages : 12 | MS Code : 2346 | Dispatch : 13-11-2020 |
|---|---|---|---|---|